

Figure S1 (related to Figure 2).

A. Data base-based identification of an intracellular TRAF6 binding site in neuroplastin tail. ELM database (<http://elm.eu.org/>) read out table showing identified binding motifs in all the mouse neuroplastin structure (top drawing). The three extracellular Ig-like domains are in green, transmembrane in blue, and intracellular tail is not colored. Note that the a single TRAF6 binding motif is identified in the cytoplasmic tail (blue square into the red frame). **B.** The table shows ELM database-based motif analysis for the listed synaptogenic cell adhesion molecules. Note that only neuroplastin display TRAF6 binding motif.

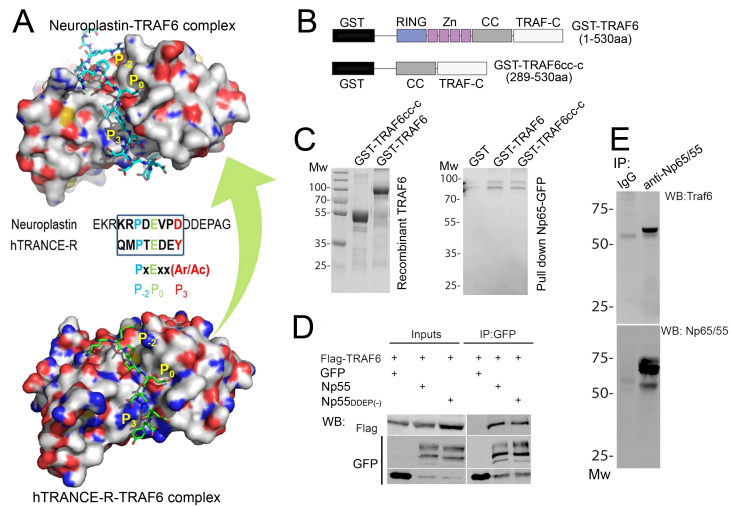


Figure S2 (related to Figure 2).

A. Modeling neuroplastin-TRAF6 binding. This model is based on the hTRANCE-R-TRAF6 interaction according to provided structures (Ye et al., 2002). The local peptide docking of the tail of neuroplastin (cyan; PBD: [1LB5_A](#)) is shown on the top and the template complex is shown below (hTRANCE-R in green; PDB: [1LB5_B](#)). Protein structure similarity (TM-score) = 0.991, Interaction similarity = 108.0, and Estimated accuracy = 0.868. Positions P₋₂, P₀ and P₃ in the TRAF6 motif are indicated in both peptide-protein complexes. Protein surfaces are colored based on element (C in white; O in red; N in blue; S in orange).

B. Representation of GST-TRAF6 and GST-coiled coil-TRAF-C domain (TRAF6_{cc-c}) recombinant proteins. RING domain, zinc fingers (Zn), coiled-coil region (CC) and C-terminal domain (TRAF-C) are indicated.

C. Left: Coomassie gel showing recombinant GST-TRAF6 and GST-TRAF6_{cc-c} recombinant proteins. Right: Western blot showing that both recombinant proteins are pulled-down by Np65-GFP from total extracts of transfected HEK cells.

D, E. Neuroplastins co-precipitate with TRAF6. The two Np55 isoforms (with and without DDEP insert) are effective to co-precipitate TRAF6 from total homogenates of transfected HEK cells (**D**). HEK cells were transfected with the indicated constructs, left to express the tagged proteins for 24 hours, and lysed with RIPA lysis buffer. The extracts were immunoprecipitated with anti-GFP antibody coupled to magnetic beads. Precipitated complexes were resolved by SDS-PAGE and immunoblotted with anti-Flag or anti-GFP antibodies. (**E**) Three-weeks old rat brains were homogenized and lysed with RIPA lysis buffer and incubated with an antibody recognizing all neuroplastin isoforms raised in rabbit (1µg/ml, Smalla et al., 2000) for 24 hours at 4°C. Precipitated

proteins were resolved by SDS-PAGE and immunoblotted with pan anti-Np65/55 antibody from sheep or anti-TRAF6 antibody from rabbit.

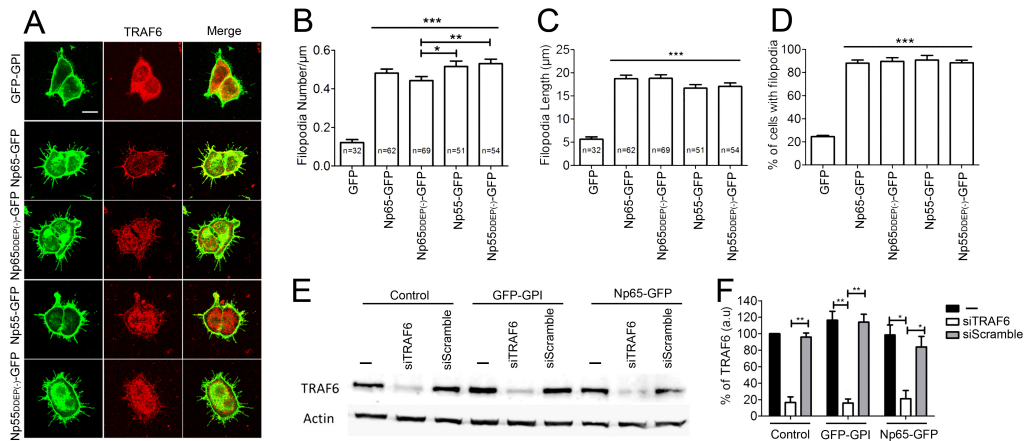


Figure S3 (related to Figure 3).

A-D. The four isoforms of neuroplastin are equally robust to promote translocation of endogenous TRAF6 to the cell membrane and to increase both number and length of filopodia. **(A)** Confocal images displaying representative examples of HEK cell transfected with different neuroplastin constructs and stained for TRAF6 as for Figure 3D. Scale bar=10 μm . **(B)** Number of filopodia (GFP=0.12 \pm 0.01 N=32; Np65-GFP=0.48 \pm 0.02 N=62; Np65_{DDEP(-)}-GFP=0.44 \pm 0.02 N=69; Np55-GFP=0.52 \pm 0.03 N=51; Np55_{DDEP(-)}-GFP=0.53 \pm 0.02 N=54) **(C)** Filopodia length (GFP=5.66 \pm 0.49; Np65-GFP=18.72 \pm 0.77; Np65_{DDEP(-)}-GFP=18.79 \pm 0.76; Np55-GFP=16.68 \pm 0.76; Np55_{DDEP(-)}-GFP=17.08 \pm 0.72) and **(D)** Percentage of cells with filopodia are displayed as mean \pm SEM. Student's t-test **(B,C)** or with Mann-Whitney test **(D)** were applied. * p <0.05, ** p <0.01, and *** p <0.001 vs GFP.

E, F. Assessment of TRAF6 knockdown efficiency upon siRNA treatment. **(E)** Total cell homogenates were resolved by SDS-PAGE and immunoblotted for endogenous TRAF6 and actin to control protein loading. **(F)** The graph shows the densitometric quantification of TRAF6 bands from three independent experiments. ** p <0.01 or * p <0.05 using Mann-Whitney test.

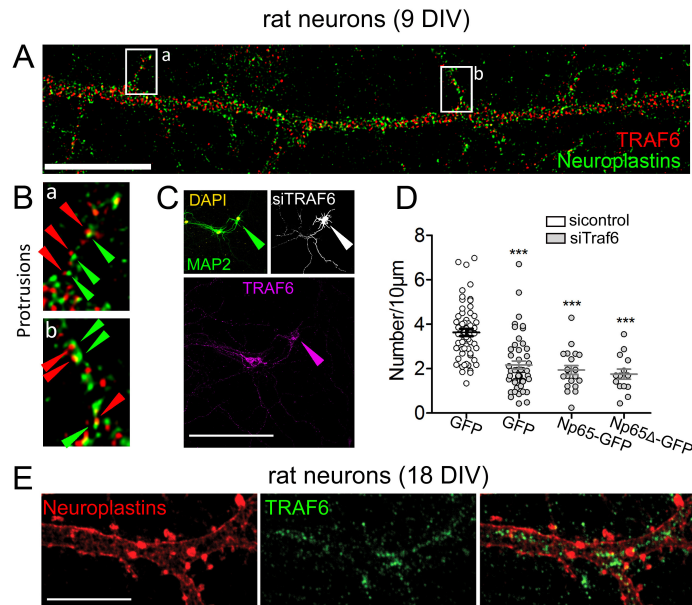


Figure S4 (related to Figure 4).

A, B. Staining of neuroplastin and TRAF6 in methanol-fixed rat young hippocampal neurons. **(A)** Neurons were stained with a pan-antibody recognizing all neuroplastin isoforms and anti-TRAF6 antibody followed by proper fluorophore-tagged secondary antibodies, mounted, and imaged using a 100x objective of a confocal microscope. Scale bar=10 μm **(B)** Digital magnification of dendritic protrusions with co-distributed and co-localized spots of neuroplastin and TRAF6 displayed. For **A** and **B**, images were deconvolved (see methods).

C, D. TRAF6 knockdown counteracts the increase of dendritic protrusions induced by Np65-GFP over-expression in hippocampal neurons. Neurons were co-transfected with either control scrambled siRNA or siRNA against TRAF6 mRNA and with GFP-encoding plasmid (6 DIV). Additionally, neurons were co-transfected with siRNA and Np65-GFP or Np65 Δ -GFP. After 72 hours, neurons were stained with anti-MAP2 and anti-TRAF6 antibodies to control neuronal morphology and TRAF6 KD, respectively. Only neurons with $\geq 60\%$ reduction in TRAF6 immunoreactivity (arrow heads) were considered for the counting of dendritic protrusions. Transfected neurons from four independent cultures were analyzed (si-control GFP=3.73 \pm 0.16 N=59; siTRAF6 GFP= 2.16 \pm 0.18 N=49; siTRAF6 Np65-GFP= 2.09 \pm 0.16 N=22; siTRAF6 Np65 Δ -GFP= 1.69 \pm 0.17 N=14). *** $p < 0.001$ vs. si-control GFP using Student's t-test. Scale bar=100 μm .

E. Neuroplastin and TRAF6 in mature hippocampal neurons. Staining was performed as in **A**. TRAF6 does not co-localize with neuroplastin in mature neurons. Scale bar=10 μm .

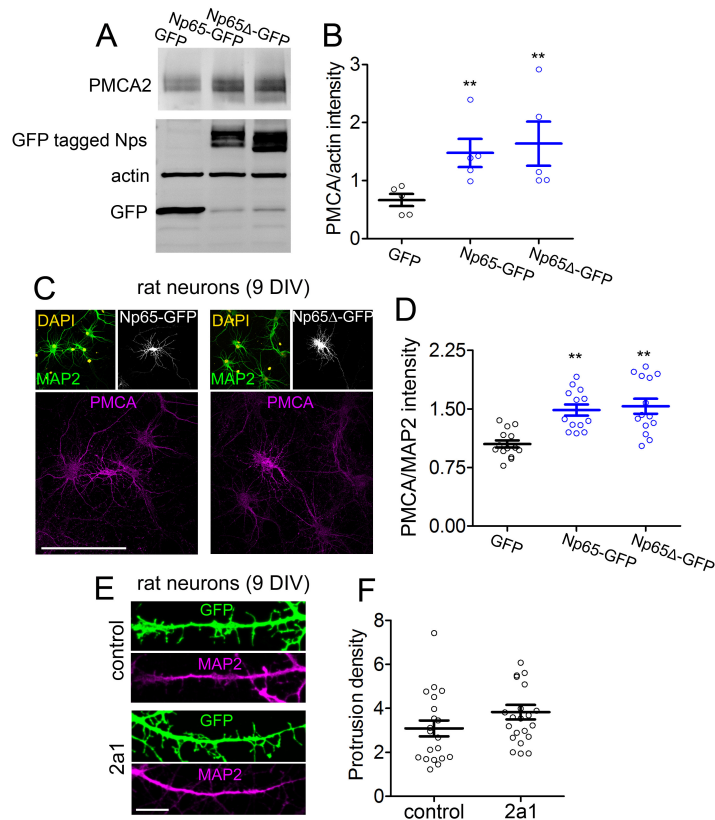


Figure S5 (related to Figure 4).

A, B. Protrusion formation does not depend on Neuroplastin-PMCA interaction. **(A)** Np65-GFP and Np65Δ-GFP equally increase total PMCA2 levels in HEK cells. Cells were transfected with the indicated constructs, harvested 24 hours later and lysed with RIPA lysis buffer. Western blot analysis shows that levels of PMCA2 are increased upon co-transfection with Np65-GFP and with Np65Δ-GFP as indicated. Blotting of actin is used to control loading. **(B)** Quantification of PMCA2 blots are normalized to actin using data from five independent experiments. **p < 0.01 vs. GFP using Mann-Whitney test.

C, D. Np65-GFP and Np65Δ-GFP lacking intracellular TRAF6 domain are equally effective to increase PMCA expression in young hippocampal neurons. **(C)** At 7DIV hippocampal neurons were transfected with plasmids encoding Np65-GFP or Np65Δ-GFP. At 9DIV, neurons were fixed and stained with an anti- MAP2 and anti-pan-PMCA antibodies. Scale bar=10 μm. **(D)** Quantification of the intensity of PMCA immunofluorescent signal normalized to MAP2 signal using data from 13-20 neurons per group from three independent cultures. **p < 0.01 vs. GFP using Student's t-test.

(GFP=1.05 ± 0.04 N=14; Np65-GFP=1.48 ± 0.07 N=13; Np65Δ-GFP= 1.53 ± 0.09 N=14).

E, F. Hippocampal neurons (DIV8) were transfected with GFP-expressing plasmid. After 24 hours, neurons were incubated with the PMCA inhibitor Caloxin 2a1, fixed, immunostained with an anti-GFP antibody and an anti-MAP2 antibody followed by proper secondary antibodies, and imaged using a confocal microscope with a 63X objective under 3X digital zoom factor. **(F)** Protrusion density in control and Caloxin 2a1 treated neurons from two independent cultures (control=3.08 ± 0.35 N=20; 2a1= 3.83 ± 0.39 N=25).